JOC The Journal of Organic Chemistry

Article

pubs.acs.org/joc

One-Shot Determination of Residual Dipolar Couplings: Application to the Structural Discrimination of Small Molecules Containing Multiple Stereocenters

Laura Castañar,[‡] Manuela Garcia,[†] Erich Hellemann,[†] Pau Nolis,[‡] Roberto R. Gil,*[,†] and Teodor Parella*[,‡]

[†]Department of Chemistry, Carnegie Mellon University, Pittsburgh, Pennsylvania 15213, United States

[‡]Servei de Ressonància Magnètica Nuclear, Universitat Autònoma de Barcelona, E-08193 Bellaterra (Barcelona), Catalonia, Spain

Supporting Information

ABSTRACT: A novel approach for the fast and efficient structural discrimination of molecules containing multiple stereochemical centers is described. A robust *J*-resolved HSQC experiment affording highly resolved $^1J_{CH}/^1T_{CH}$ splittings along the indirect dimension and homodecoupled ^1H signals in the detected dimension is proposed. The experiment enables in situ distinction of both isotropic and anisotropic components of molecules dissolved in compressed PMMA gels, allowing a rapid and direct one-shot determination of accurate residual dipolar coupling constants from a single NMR spectrum.

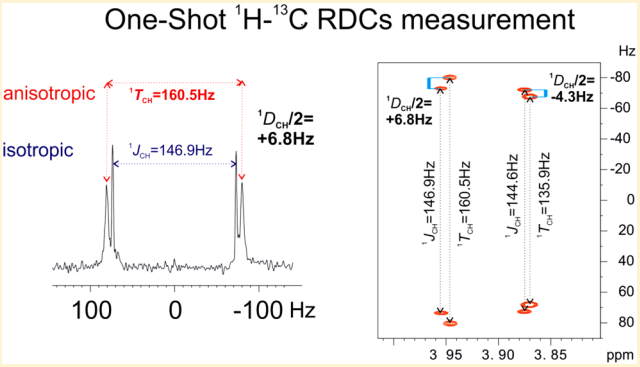

INTRODUCTION

NMR spectroscopy in anisotropic media is becoming a very powerful tool for the structural analysis of small organic molecules of natural and synthetic origin. This emerging NMR technique started to show its power to determine the constitution, the relative configuration as well as the preferred conformation of small molecules with the first reports in the earlier 2000.[1−6] Since then, two major groups of alignment media were developed including strained aligning gels (SAG) in stretching and compression mode[7−12] and lyotropic liquid crystalline (LLC) phases of helical polymers, such as poly-γ-benzyl-L-glutamate (PBLG), poly-γ-ethyl-L-glutamate (PELG), poli-ε-carbobenciloxi-L-lisina (PCBLL), polyacetylenes, polyisocyanides, or graphene oxides.[13−16] In 2008, the Gil's group reported the use of stretched poly(methyl methacrylate) (PMMA) gels as alignment media compatible with $CDCl_3$[10] in addition to the already existing aligning gels developed by Luy's group.[7−9,12] At that time, the only existing method was to let gels sticks (4 mm in diameter and 10 mm of length) to swell and self-stretch in 5 mm NMR tubes using the NMR tube wall as constriction for the swelling. The swelling time to reach equilibrium was extremely slow (~30 days) and the diffusion of the sample into the gel took about 48 h. Many small molecules were partially aligned in different type of gels using this swelling method and their structures were solved using residual dipolar couplings (RDCs). Later in 2010, Gil's group developed a new tunable and faster method, based on reversible compression/relaxation of flexible PMMA gels.[11] In this method, 2 mm in diameter and 25 mm-long gels were swollen in few hours and sample was diffused into the gels in a matter of minutes. In contrast to stretched gels and LLC phases, it is not possible to avoid the presence of some residual isotropic environment between the wall of the tube and the gel in compressible PMMA gels. As the gel is further compressed, the amount of isotropic contribution is minimized but not totally eliminated.

RDCs ($^1D_{CH}$) are calculated from the difference in splitting between the signals separately collected in isotropic ($^1J_{CH}$) and anisotropic conditions ($^1T_{CH}$ = $^1J_{CH}$+$^1D_{CH}$). The conventional measurement from the F_2 dimension of an HSQC spectrum takes advantage of the ease with which one can obtain high levels of digital resolution and recently, broadband homodecoupled versions have been proposed to simplify the multiplet structure, allowing the precise measurement with a simple peak analysis.[17−20] Unfortunately, these promising methods require a time-consuming 3D acquisition mode and, on the other hand, the interference of J_{HH} splitting, proton dipolar coupling broadening and strong coupling effects can be more than enough reasons to avoid any F_2 ^1H-coupled HSQC experiments to measure RDCs when using compressible gels method. In addition, the overlapping of the isotropic and anisotropic components can lead to RDCs with higher errors. Alternatively, different approaches have been proposed to measure them from the indirect F_1 dimension, being the *J*-scaled BIRD (bilinear rotation decoupling) HSQC (referred to as JSB-HSQC) chemical shift correlation experiment the most

Received: August 25, 2016
Published: October 6, 2016

DOI: 10.1021/acs.joc.6b02103
J. Org. Chem. 2016, 81, 11126−11131

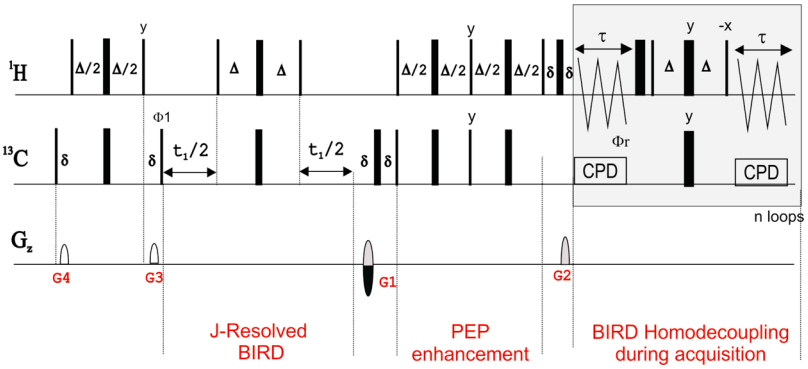

Figure 1. Homodecoupled *J*-resolved HSQC (HD-*J*-HSQC) pulse sequence to measure $^{1}J_{CH}/^{1}T_{CH}$ in small molecules at natural abundance. Narrow and wide filled bars correspond to 90° and 180° pulses, respectively, with phase x unless indicated otherwise. All inversion and refocusing 180° ^{13}C pulses can be applied as adiabatic shaped pulses. The interpulse delay in INEPT and BIRD elements are set to $\Delta = 1/(2^{*1}J_{CH})$. Coherence order selection and echo−antiecho phase sensitive detection in the ^{13}C-dimension are achieved with gradient pulses G1 and G2 in the ratio of 80:20.1. During the BIRD-based acquisition period, the first and last chunks are half the duration (τ = AQ/2n) of the remaining chunks (AQ/n). A basic two-step phase cycle is used: ϕ_1 = x,−x and ϕ_{rec} = x,−x.

suitable tool.[21−23] In this case, the interference of J_{HH}/D_{HH} is avoided and long-range heteronuclear contributions are efficiently minimized by using a BIRD module inserted into the t_1 period. Experimentally, the major inconvenience is that an elevate number of t_1 increments is strongly required to obtain reasonable resolution levels along F_1, considerably increasing the overall acquisition time. We propose here a robust modification of the reference JSB-HSQC experiment by introducing different features that significantly enhance sensitivity, digital and signal resolution, facilitate spectral analysis and automated extraction of coupling values, and speed up data acquisition. It will be shown that both isotropic ($^{1}J_{CH}$) and anisotropic ($^{1}T_{CH}$) components can be simultaneously observed into the same NMR spectrum, allowing the direct determination of both the sign and the magnitude of RDCs from a single measurement.

RESULTS AND DISCUSSION

Figure 1 displays the pulse scheme of the homodecoupled *J*-resolved HSQC (HD-*J*-HSQC) experiment proposed for the fast and straightforward measurement of precise *J*/*T* values. This novel method (i) uses an exclusive J_{CH}-evolution t_1 period where a central BIRD element refocuse any long-range CH coupling and ^{13}C chemical shift evolutions,[24−26] (ii) the sensitivity is enhanced mainly for CH spin systems using the classical preservation of equivalent pathways (PEP) technique,[27] (iii) real-time BIRD-based homodecoupling during acquisition is implemented using the recent data chunk approach,[28] and (iv) nonuniform sampling (NUS)[29] can reduce spectrometer time while keeping high levels of digital resolution in the F_1 dimension. The use of a *J*-resolved format instead to the classical *J*-scaled $\delta(^{13}C)$ correlation map offers important advantages, as reported for visualizing enantiomers using chiral liquid crystals.[25] First, the evolution of the ^{13}C transverse magnetization is reduced to a single period, avoiding the use of an extra incrementable delay for $\delta(^{13}C)$ evolution and also of unnecessary *J* scaling factors (κ) that increase in a counterproductive way t_1^{max}. Second and fundamental for our purpose, digital resolution per time unit along the F_1 dimension is largely improved by a factor of ∼40, as shown for an isotropic sample of estradiol in the SI (Figures S2−S4). For instance, typical parameters to run a HD-*J*-HSQC with 16 scans, 256 increments in F_1, a spectral window in F_1 of 500 Hz (FID resolution of 3.9 Hz/Pt), took 1 h 37 min to complete, while the equivalent JSB-HSQC (with same number of scans, 1024 increments in F_1, spectral window in F_2 of 20120 Hz/160 ppm, FID resolution of 39.3 Hz/Pt) took 5 h and 58 min to complete. In other words, HD-*J*-HSQC offers spectrometer time savings by a factor of 4 whereas resolution is enhanced by a factor of ∼10. In addition, the use of NUS can improve even more the digital resolution per time unit without hardly affecting spectral quality. For instance, the equivalent spectrum could be obtained with only ∼25 min using 25% NUS (Figures S5−S7). Also noteworthy, the symmetrical responses around the F_1 = 0 axis expedite spectral analysis besides facilitating the extraction of $^{1}J_{CH}$ coupling splitting using automated algorithms (see SI). The only limitation of these *J*-resolved methods (as opposed to F_1 coupled HSQC) in that removal of the ^{13}C chemical shift dispersion can generate some accidental overlap. In such particular cases, the proposed experiment could also be recorded with ^{13}C chemical shift evolution, similarly as reported in ref 21−23 (see Figure S1).

On the other hand, the addition of homodecoupling features in HD-*J*-HSQC introduces a significant degree of simplification in the splitting patterns of ^{1}H resonances in F_2, as shown for an isotropic sample of strychnine (**1**) in Figure 2. Multiplets containing only $^{3}J_{HH}$ and long-range $^{n}J_{HH}$ couplings literally collapse into singlets, while protons belonging to CH_2 groups maintain the $^{2}J_{HH}$ coupling. This is due to the fact that the BIRD decoupling scheme in the acquisition decouples protons attached to ^{13}C from protons attached to ^{12}C. Since CH_2 protons are attached to the same ^{13}C atom are not fully decoupled. In terms of sensitivity, the averaged experimental signal-to-noise ratio (SNR) for CH and CH_2 groups after homodecoupling is enhanced by a factor of 2.15 and 1.59, respectively, which is in accordance with the corresponding complete and partial signal collapsing reported by real-time BIRD-based homodecoupling in other HSQC-like experiments.[28] As predicted theoretically, the PEP approach (optimized for CH systems) also affords an additional gain of 1.37 for CH whereas CH_2 is decreased by 0.82 (Figure S8). In summary, the overall sensitivity gain factors for both PEP and homodecoupling contributions are averaged to 2.97 and 1.29 for CH and CH_2, respectively. (Figure 2C vs 2D).

The usefulness of all these significant technological improvements is here illustrated by solving a real challenging case of

DOI: 10.1021/acs.joc.6b02103
J. Org. Chem. 2016, 81, 11126−11131

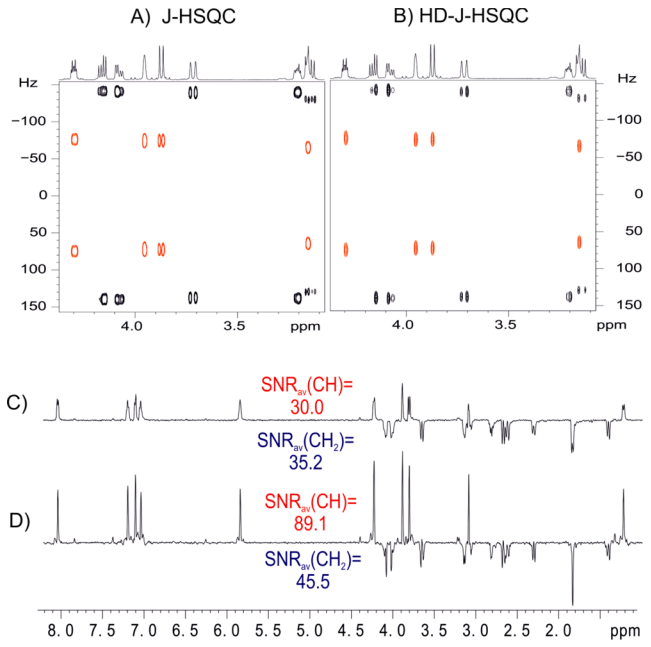

Figure 2. 600.13 MHz (A) Conventional and (B) homodecoupled *J*-HSQC spectra of strychnine (**1**) in isotropic $CDCl_3$, both acquired under the same experimental conditions. (C−D) Internal F_2 projections extracted from spectra A and B, respectively, with the corresponding average SNR values for CH (up) and CH_2 (down) resonances. In (D) the accumulative benefits of both PEP and homodecoupling enhancements are considered.

severe ^{1}H signal overlap. It is shown how nearly identical set of signals corresponding to the molecules outside the gel (isotropic component) and inside the gel (anisotropic component) can be unraveled in a weakly aligned molecular sample, all they having complex *J* coupling patterns and broad line widths, particularly those signals from the anisotropic environment. The enormous potential of the HD-*J*-HSQC experiment for the efficient, fast and simultaneous measurement of both $^1J_{CH}$ and $^1T_{CH}$ in compressed anisotropic gels is demonstrated for two reference molecules, strychnine (**1**)[22] and ludartin (**2**),[10] which have been already tested in other related works. Figure 3A shows the HD-*J*-HSQC spectrum of **1** dissolved in a compressed PMMA/$CDCl_3$ gel ($CDCl_3$ ^{2}H quadrupolar splitting of $\Delta\nu_Q$ = 33.4 Hz). Under such conditions, the beauty is the observation of well-defined doublets in F_1 for all cross-peaks corresponding to the isotropic ($^1J_{CH}$) and anisotropic ($^1T_{CH}$) components, allowing the direct determination of both the sign and the magnitude of RDCs from a single sample and a single NMR data set (Figures 3B, 4, and S9−S12). This idea has been already described using a DMSO-compatible polymethacrylate-based aligned gel showing very large chemical shift dispersion between the isotropic and anisotropic components (0.1 ppm).[30] We show here that the strikingly high degree of resolution in HD-*J*-HSQC allows very precise measurements even in the case of degenerate ^{1}H chemical shifts, where related F_2-coupled HSQC experiments would fail completely. The relative shifts of isotropic vs anisotropic ^{1}H signals in F_2 can be either positive or negative, spread out over a short-range of $\Delta\delta(^1H)$= ± 22 ppb (±13 Hz @ 600 MHz) (Figure 4) and they could be a good indicator about small ^{1}H residual chemical shift anisotropy (RCSA) effects (not evaluated in this work). Although they should still be necessary to use the isotropic spectrum as a control experiment for a unambiguous assignment, the different line widths and the relative signal intensities can be used for unequivocally distinguishing the corresponding isotropic and anisotropic components. As known, the central lines corresponding to the theoretical doublet of doublets in F_1 of CH_2 cross peaks are missing in HD-*J*-HSQC spectra and, therefore, only the sum of $^1J_{CHa}$ + $^1J_{CHb}$ are obtained for diastereoptopic CH_aCH_b spin systems. Fortunately, it has been previously shown that it is not necessary to assign the diastereotopic CH_2 protons for the RDC-assisted structural discrimination process if the sums of the couplings of each individual C−H bond in these methylene groups are used in the SVD fitting of data to structure.[23,31−33] We were able to determine all ^{1}H−^{13}C RDCs except for H22 (<1 Hz), which was not relevant in subsequent calculations. The goodness of the method is accomplished by the exceptional level of structural discrimination achieved between eight possible diastereoisomeric configurations of **1** using the MSpin program (Tables S1−S3).[34] Our single HD-*J*-HSQC data in the form of quality factors (*Q*) are in very good agreement with those previously reported with two-measurement JSB-HSQC (*Q* factors of 0.061 vs 0.054 using molecular mechanics (MMFFs) for the correct structure and of 0.118 vs 0.115 for the second lowest *Q* corresponding to the C12 epimer).[23] The *Q* factor is further improved using DFT-level calculated structures (0.031 vs 0.045, respectively). These results significantly improve other related RDC data reported on **1** that include long-range CH couplings (*Q* factors of 0.086 with only $^1D_{CH}$ and 0.090 including $^nD_{CH}$)[35] and RCSA (^{13}C) (*Q* factors of 0.050 and 0.071 using DFT structures with stretching and compression methods, respectively) restraints.[36] The major advantages of our proposal are sustained on three main factors: (i) the greater speed with which the data are collected, (ii) the precise measurement due to the high resolution achieved along the F_1 dimension and the peak simplification obtained by homodecoupling (Figure 4), and (iii) the efficient minimization of errors by avoiding two different measurements.

Far from being a drawback, the coexistence of isotropic and anisotropic contributions offers an unprecedented scenario in the fast and accurate determination of RDCs. As another proof of concept we provide the RDC results obtained for **2** dissolved in a compressed PMMA gel swollen in $CDCl_3$ ($\Delta\nu_Q$ = 33.6 Hz) in which the configuration of its epoxide ring was unambiguously solved using only RDCs.[10] $^1D_{CH}$ RDCs were measured for every CH pair in the molecule. Average values were measured for methyl groups and sum of couplings ($^1D_{CHa}$+$^1D_{CHb}$) for methylenes. The Table S4 compiles all RDC values collected with the homodecoupled versions of the JSB-HSQC and *J*-HSQC experiments (Figures 5 and S13). Structures for both epimers of the 3,4-epoxide group were generated at different levels of theory (molecular mechanics, AM1 and DFT) and SVD fitting results of the RDC data to these structures are shown along with all *Q* factors in Table 1. The best degree of configuration discrimination is achieved with the data collected with HD-*J*-HSQC and using the structures generated by DFT, with definitive *Q* factors of 0.031 for the correct structure and 0.239 for the wrong one.

■ CONCLUSIONS

Since the first report on the use of aligning gels compatible with organic solvents, within the last years there was an exponential degree of improvement in all the fronts of the methodological aspect to measure $^1D_{CH}$ RDCs at ^{13}C natural abundance. We

DOI: 10.1021/acs.joc.6b02103
J. Org. Chem. 2016, 81, 11126−11131

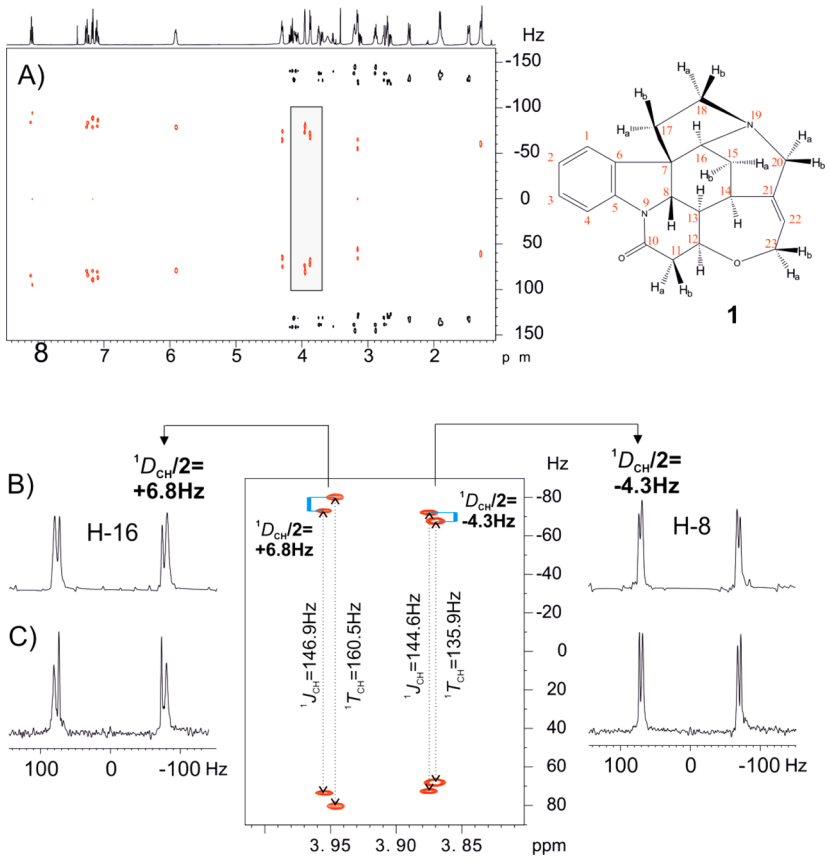

Figure 3. (A) HD-*J*-HSQC spectrum of **1** in compressed PMMA/$CDCl_3$ (^2H quadrupolar coupling ($CDCl_3$) = 33.4 Hz). (B, C) Expanded region and selected 1D columns corresponding to the H-16 and H-8 protons (marked box in A) showing how $^1J_{CH}$, $^1T_{CH}$, and $^1D_{CH}$ can be measured simultaneously with high precision for each resolved peak. Experimental details: spectral width in F_1 = 4 ppm, number of complex data points in F_2 = 2048, number of t_1 increments = 512, NUS = 25%, FID resolution = 2.35 Hz, number of scans = 4, relaxation delay = 1 s, experimental time = 11 min 34 s, spectral resolution after zero filling to 2k in F_2 = 0.29 Hz. Data acquisition was divided into 16 chunks with τ = 10.3 ms each. 1D columns correspond to the H-16 and H-8 protons in equivalent (B) 25% non-uniform (acquired in 11 min 13 s) and (C) uniform (acquired in 53 min 13 s) sampling data sets are shown for visualize the NUS effect.

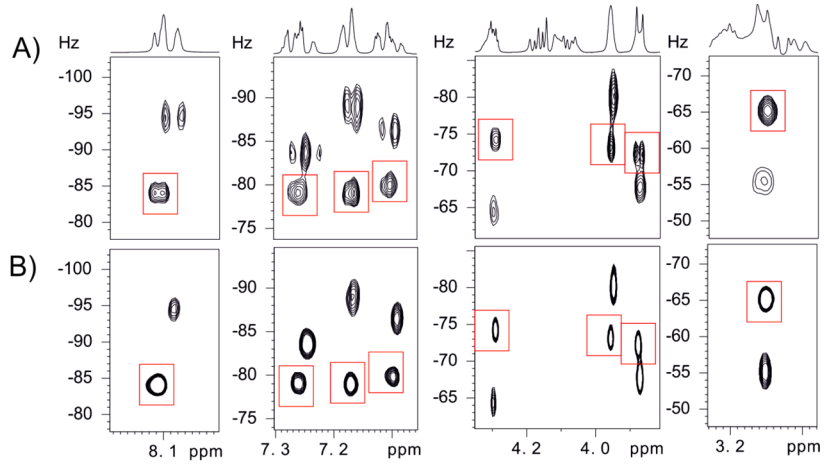

	H4	H3	H1	H2	H12	H16	H8	H14
$^1D_{CH}$ (Hz)=	+20.6	+8.6	+19.6	+12.3	-20.5	+13.6	-8.7	-19.3
$\Delta\delta(^1H)$ (Hz)=	-12.8	-7.9	-3.0	-5.3	+4.0	-3.7	-2.3	+3.2
$\Delta\delta(^1H)$ (ppb)=	-21.4	-13.6	-5.0	-9.0	+6.8	-6.3	-3.7	+5.3

Figure 4. Comparison of some selected upfield cross-peaks from the (A) regular and (B) HD-*J*-HSQC spectra of **1** in compressed PMMA/$CDCl_3$. Note that a simple peak distance measurement can afford directly the sign and the magnitude of $^1D_{CH}$ (in Hz) as well as the corresponding $\Delta\delta(^1H)$ values (in Hz and ppb). Isotropic components are readily identified as sharper signals and marked into red boxes.

DOI: 10.1021/acs.joc.6b02103
J. Org. Chem. 2016, 81, 11126−11131

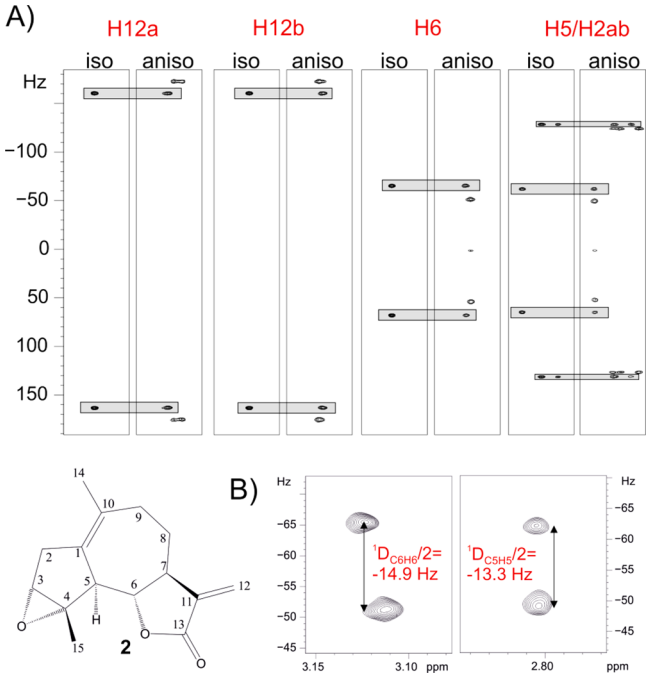

Figure 5. HD-*J*-HSQC spectra of **2** in isotropic ($CDCl_3$) and anisotropic (PMMA/$CDCl_3$) conditions. Note how the isotropic signal in both isotropic and anisotropic spectra present the same experimental $^1J_{CH}$ splitting, confirming its use as an internal reference to determine directly the sign and the magnitude of $^1D_{CH}$ in the anisotropic sample.

Table 1. Quality Factors (Q) from the Fittings of RDC Data to the Structure of the 3,4-Epoxide Epimers of Ludartin (2)[a]

compound	Q factor JSB-HSQC (MM)	Q factor HD-J-HSQC (MM)	Q factor JSB-HSQC (AM1)	Q factor HD-J-HSQC (AM1)	Q factor JSB-HSQC (DFT)	Q factor HD-J-HSQC (DFT)
3,4-epi-ludartin	0.223	0.213	0.243	0.245	0.240	0.239
ludartin (**2**)	0.150	0.112	0.143	0.115	0.052	0.031

[a]MM: Molecular mechanics (MMFFs); AM1: semiempirical method; DFT: density functional theory.

believe that by introducing homodecoupling in combination with *J*-resolved mode into the HSQC experiment we made another quantum leap in the methodology. It has been shown that the combination of several resolution enhancement techniques into a single HD-*J*-HSQC experiment introduces substantial improvements in spectral quality, sensitivity, and both signal and digital resolution. This is a good example showing that RDCs of variable size and sign can be precisely determined from a single NMR spectrum, minimizing typical errors of measuring them from two different sample conditions. In addition, the simple representation of the *J*-resolved format opens new avenues toward an automated analysis and quantitative extraction of *J* and *D* coupling values. The advances in sample preparation, faster data collection and better measurement accuracy will make the determination and therefore the application of RDCs to solve structural, configurational, and conformational aspects in small molecules more efficient, affordable, and easier, even for nonexperienced users.

EXPERIMENTAL SECTION

NMR experiments were recorded on a 600 MHz spectrometer equipped with a triple-resonance $^1H/^{13}C/BB$ inverse probe for the samples of strychnine (**1**) and estradiol (**3**), and on a 500 MHz spectrometer equipped with a broadband inverse probe for the samples of ludartin (**2**). The temperature for all measurements was set to 298 K. The isotropic samples were similarly prepared by dissolving 20 mg of **1** in $CDCl_3$ and **3** in DMSO-d_6. Anisotropic samples were prepared as described in ref 22 of the manuscript. They consisted of 20 mg of **1**, 2.7 mg of **2**, and 20 mg of **3** aligned in a poly(methyl methacrylate) (PMMA) gel swollen in $CDCl_3$ using the reversible compression/relaxation method. The ^2H quadrupolar splitting ($\Delta\nu_Q$) for the $CDCl_3$ signal was set to 33.4 Hz for the anisotropic samples of **1** and **2**.

NMR spectra of samples **1** and **3** were recorded with proton 90° pulses of 8.5 μs and carbon 90° pulses of 10.5 μs. For broadband carbon inversion and refocusing, 0.5 ms smoothed Chirp pulses sweeping over a frequency band of 60 kHz and a four-Chirp composite pulse of 2 ms duration were used, respectively. For a precise comparison, all nonhomodecoupled and homodecoupled JSB-HSQC and *J*-HSQC experiments were generally recorded with the same acquisition and processing parameters if otherwise is indicated. The interpulse Δ delays in INEPT and BIRD elements were set to 3.5 ms ($\Delta = 1/(2*^1J_{CH})$; optimized to $^1J_{CH}$ = 145 Hz) and the recycle delay to 1 s. Gradient ratios for G1:G2:G3:G4 were set to 80:20.1:13:23, measured as percentage of the absolute gradient strength of 53.5 G/cm. Sine bell shaped gradients had 1 ms of duration and were followed by a recovery delay of 100 μs (δ). All experiments were acquired and processed using the echo/antiecho protocol where the gradient G1 was inverted for every second FID. Real-time BIRD-based homodecoupling was performed using 10.3 ms chunk length and 8 loops (2048 complex points in F_2).

General conditions for the *J*-HSQC experiment on **1**: 2 scans were accumulated for each one of the 512 t_1 increments and the number of complex data points in t_2 was set to 2048. Spectra were acquired with an spectral window of 6000 Hz (in F_2) and 600 Hz (in F_1) giving a FID resolution of 5.8 (F_2) and 2.34 (F_1) Hz, respectively. Prior to Fourier-transformation of each data, zero filling to 2048 in F_1 and a π/2-shifted squared cosine window function (QSINE, SSB: 2) in both dimensions were applied. After applying zero filling the digital resolution was 2.93 (F_2) and 0.1 (F_1) Hz, respectively. Similar conditions were used to collect JSB-HSQC experiments, changing only the spectral width in the indirect F_1 dimension to 160 ppm (24000 Hz) and the *J*-scaling factor to k = 1−8. The FID resolution was of 5.8 (F_2) and 94.3 (F_1) Hz, respectively. The *J*-HSQC experiments on **2** were acquired with 85 scans, an acquisition matrix of 1k (F_2)*256 (F_1) and processed with zero-filling to 4k*4k.

The 3D structures of all compounds were initially generated using the MacroModel Suite from Shrödinger (https://www.schrodinger.com/MacroModel/). The diastereomers were automatically generated using the LigPrep module in MacroModel and further energy minimized using the MMFFs molecular mechanics force field. AM1 and DFT (B3LYP/6-31G*) calculations were performed in Gaussian 09 (http://www.gaussian.com) .

Fitting of RDC data to structures was performed using the MSpin software package (Mestrelab Research S.L., Santiago de Compostela, Spain). http://www.mestrelab.com.

The java applet jmeasurement.jar described at the end of this SI for extracting $^1J_{CH}$ automatically from a previous peak picking file is available on request.

ASSOCIATED CONTENT

Supporting Information

The Supporting Information is available free of charge on the ACS Publications website at DOI: 10.1021/acs.joc.6b02103.

Complete set and expanded NMR spectra of compounds strychnine (**1**), ludartin (**2**), and estradiol (**3**) comparing and showing the different experimental features

DOI: 10.1021/acs.joc.6b02103
J. Org. Chem. 2016, 81, 11126−11131

described in the manuscript, and tables with experimental and calculated RDCs data (PDF)

AUTHOR INFORMATION

Corresponding Authors

*E-mail: rgil@andrew.cmu.edu

*E-mail: teodor.parella@uab.cat

Notes

The authors declare no competing financial interest.

ACKNOWLEDGMENTS

Financial support for this research provided by Spanish MINECO (project CTQ2015-64436-P) is gratefully acknowledged. We also thank to the Servei de Ressonància Magnètica Nuclear, Universitat Autònoma de Barcelona, for allocating instrument time to this project. NMR instrumentation at Carnegie Mellon University was partially supported by the NSF (CHE-0130903 and CHE-1039870). R.R.G. gratefully acknowledges support from the NSF (CHE-1111684).

REFERENCES

(1) Thiele, C. M. *Concepts Magn. Reson., Part A* **2007**, *30A*, 65−80.

(2) Thiele, C. M. *Eur. J. Org. Chem.* **2008**, *2008*, 5673−5685.

(3) Kummerlöwe, G.; Luy, B. *Annu. Rep. NMR Spectrosc.* **2009**, *68*, 193−232.

(4) Gil, R. R. *Angew. Chem., Int. Ed.* **2011**, *50*, 7222−7224.

(5) Gil, R. R.; Griesinger, C.; Navarro-Vázquez, A.; Sun, H. In *Structure Elucidation in Organic Chemistry*; Wiley-VCH Verlag GmbH & Co. KGaA, 2015; pp 279−324.

(6) Gil, R. R. In *Reference Module in Chemistry, Molecular Sciences and Chemical Engineering*; Elsevier Inc., 2016. 10.1016/B978-0-12-409547-2.12127-4.

(7) Kobzar, K.; Kessler, H.; Luy, B. *Angew. Chem., Int. Ed.* **2005**, *44*, 3145−3147.

(8) Freudenberger, J. C.; Knör, S.; Kobzar, K.; Heckmann, D.; Paululat, T.; Kessler, H.; Luy, B. *Angew. Chem., Int. Ed.* **2005**, *44*, 423−426.

(9) Luy, B.; Kobzar, K.; Knör, S.; Furrer, J.; Heckmann, D.; Kessler, H. *J. Am. Chem. Soc.* **2005**, *127*, 6459−6465.

(10) Gil, R. R.; Gayathri, C.; Tsarevsky, N. V.; Matyjaszewski, K. *J. Org. Chem.* **2008**, *73*, 840−848.

(11) Gayathri, C.; Tsarevsky, N. V.; Gil, R. R. *Chem. - Eur. J.* **2010**, *16*, 3622−3626.

(12) Merle, C.; Kummerlöwe, G.; Freudenberger, J. C.; Halbach, F.; Stöwer, W.; Gostomski, C. L. V.; Höpfner, J.; Beskers, T.; Wilhelm, M.; Luy, B. *Angew. Chem., Int. Ed.* **2013**, *52*, 10309−10312.

(13) Courtieu, J.; Lesot, P.; Meddour, A.; Merlet, D.; Aroulanda, C. *eMagRes.* **2002**, *1*, 578−586.

(14) Luy, B. *J. Indian Inst. Sci.* **2010**, *90*, 119−132.

(15) Zong, W.; Li, G. W.; Cao, J. M.; Lei, X.; Hu, M.-L.; Sun, H.; Griesinger, C.; Tan, R. X. *Angew. Chem., Int. Ed.* **2016**, *55*, 3690−3693.

(16) Lei, X.; Xu, Z.; Sun, H.; Wang, S.; Griesinger, C.; Peng, L.; Gao, C.; Tan, R. X. *J. Am. Chem. Soc.* **2014**, *136*, 11280−11283.

(17) Timári, I.; Kaltschnee, L.; Kolmer, A.; Adams, R. W.; Nilsson, M.; Thiele, C. M.; Morris, G. A.; Kövér, K. E. *J. Magn. Reson.* **2014**, *239*, 130−138.

(18) Reinsperger, T.; Luy, B. *J. Magn. Reson.* **2014**, *239*, 110−120.

(19) Kaltschnee, L.; Kolmer, A.; Timari, I.; Schmidts, V.; Adams, R. W.; Nilsson, M.; Köver, K. E.; Morris, G. A.; Thiele, C. M. *Chem. Commun.* **2014**, *50*, 15702−15705.

(20) Timári, I.; Kaltschnee, L.; Raics, M. H.; Roth, F.; Bell, N. G. A.; Adams, R. W.; Nilsson, M.; Uhrín, D.; Morris, G. A.; Thiele, C. M.; Kövér, K. E. *RSC Adv.* **2016**, *6*, 87848−87855.

(21) Fehér, K.; Berger, S.; Kövér, K. E. *J. Magn. Reson.* **2003**, *163*, 340−346.

(22) Thiele, C. M.; Bermel, W. *J. Magn. Reson.* **2012**, *216*, 134−143.

(23) Snider, J. D.; Troche-Pesqueira, E.; Woodruff, S. R.; Gayathri, C.; Tsarevsky, N. V.; Gil, R. R. *Magn. Reson. Chem.* **2012**, *50*, S86−S91.

(24) Liu, M. L.; Farrant, R. D.; Gillam, J. M.; Nicholson, J. K.; Lindon, J. C. *J. Magn. Reson., Ser. B* **1995**, *109*, 275−283.

(25) Ziani, L.; Courtieu, J.; Merlet, D. *J. Magn. Reson.* **2006**, *183*, 60−67.

(26) Saurí, J.; Castañar, L.; Nolis, P.; Virgili, A.; Parella, T. *J. Magn. Reson.* **2014**, *242*, 33−40.

(27) Kay, L. E.; Keifer, P.; Saarinen, T. *J. Am. Chem. Soc.* **1992**, *114*, 10663−10665.

(28) Paudel, L.; Adams, R. W.; Király, P.; Aguilar, J. A.; Foroozandeh, M.; Cliff, M. J.; Nilsson, M.; Sándor, P.; Waltho, J. P.; Morris, G. A. *Angew. Chem., Int. Ed.* **2013**, *52*, 11616−11619.

(29) Mobli, M.; Hoch, J. C. *Prog. Nucl. Magn. Reson. Spectrosc.* **2014**, *83*, 21−41.

(30) Gil-Silva, L. F.; Santamaría-Fernández, R.; Navarro-Vázquez, A.; Gil, R. R. *Chem. - Eur. J.* **2016**, *22*, 472−476.

(31) Ottiger, M.; Delaglio, F.; Marquardt, J. L.; Tjandra, N.; Bax, A. *J. Magn. Reson.* **1998**, *134*, 365−369.

(32) Losonczi, J. A.; Andrec, M.; Fischer, M. W.; Prestegard, J. H. *J. Magn. Reson.* **1999**, *138*, 334−342.

(33) Trigo-Mouriño, P.; Santamaría-Fernández, R.; Sánchez-Pedregal, V. M.; Navarro-Vázquez, A. *J. Org. Chem.* **2010**, *75*, 3101−3104.

(34) Navarro-Vazquez, A. *Magn. Reson. Chem.* **2012**, *50*, S73−S79.

(35) Nath, N.; d'Auvergne, E. J.; Griesinger, C. *Angew. Chem., Int. Ed.* **2015**, *54*, 12706−12710.

(36) Nath, N.; Schmidt, M.; Gil, R. R.; Williamson, R. T.; Martin, G. E.; Navarro-Vázquez, A.; Griesinger, C.; Liu, Y. *J. Am. Chem. Soc.* **2016**, *138*, 9548−9556.

DOI: 10.1021/acs.joc.6b02103
J. Org. Chem. 2016, 81, 11126−11131